Truncated Painlevé Expansion – A Unified Approach to Exact Solutions and Dromion Interactions of (2+1)-Dimensional Nonlinear Systems

Ramaswamy Radha[a,b,c], Xiao Yan Tang[a], and Sen Yue Lou[a,c]

[a] Department of Physics, Shanghai Jiao Tong University, Shanghai, 200030, China
[b] Department of Physics, Govt. College for Women, Kumbakonam-612001, India
[c] Center of Nonlinear Science, Ningbo University, Ningbo, 315211, China

Reprint requests to R. R.; E-mail: radha_rawaswamy@yahoo.com

Z. Naturforsch. **62a,** 107 – 116 (2007); received November 15, 2006

In this paper, we formulate a method wherein we harness the results of the Painlevé analysis to generate the solutions of the (2+1)-dimensional Ablowitz-Kaup-Newell-Segur system completely in terms of the arbitrary functions. This method is mainly based on the results of the truncated Painlevé expansion. Different types of interactions among dromions are deeply understood both analytically and numerically. Especially, different from the traditional viewpoint, we point out that the soliton (dromion) fission and fusion may be an approximate phenomenon.

Key words: Truncated Painlevé Expansion; Exact Solutions; Dromion Interactions.

1. Introduction

The recent spurt in the study of integrable models in (2+1)-dimensions is mainly attributed to the identification of dromions [1 – 4] which decay exponentially in all directions. These dromions which exist at the point of intersection of two ghost solitons can be driven anywhere in the two-dimensional plane by suitably choosing the boundaries. Can one generate solutions which are more general than the exponentially localized solutions just as the one-dimensional solitons happen to be the special case of the doubly periodic Jacobian elliptic functions? How can they be generated? The primary objective of this paper is to make a nascent contribution in this direction to answer the above questions.

It is known that for higher dimensional soliton systems, there are abundant localized excitations and rich interaction phenomena. Especially, the interactions among dromions may be completely elastic in some cases and completely inelastic in some other cases. When the interaction is inelastic, two dromions may exchange some physical quantities or even completely exchange their shapes. Even though the fact that one dromion may split into two [5] and two or more dromions may fuse together to form a single dromion [6] is already known, one does not really know the criterion behind the fission and fusion of dromions. In this paper, we take a typical two-dromion solution of the Ablowitz-Kaup-Newell-Segur (AKNS) system as a simple example to give a clear picture on the dromion interaction.

2. (2+1)-Dimensional AKNS System

The (2+1)-dimensional AKNS system is one of the most important dynamical systems arising in various physical situations [7 – 9] and is given by

$$\mathrm{i}q_t + q_{xx} + q_{yy} - 2\lambda q(U+V) = 0, \tag{1}$$

$$-\mathrm{i}r_t + r_{xx} + r_{yy} - 2\lambda r(U+V) = 0, \tag{2}$$

$$V_x = (qr)_y \; [\text{or } V = \int (qr)_y \mathrm{d}x + V_2(y,t)], \tag{3}$$

$$U_y = (qr)_x \; [\text{or } U = \int (qr)_x \mathrm{d}y + U_2(x,t)], \tag{4}$$

where q and r are the complex physical fields, and V and U are the potentials. The above equation system (1) – (4) reduces to the Davey-Stewartson (I) equation [10] under the reduction $r = q^*$. Expanding the physical fields and the potentials in the form of a Laurent series in the neighbourhood of a noncharacteristic manifold $\phi(x,y,t) = 0$ and utilizing the results of the Painlevé test admitted by the above equation [11, 12], we obtain the following Bäcklund transformation by truncating at the constant level term:

$$q = \frac{q_0}{\phi} + q_1, \tag{5}$$

$$r = \frac{r_0}{\phi} + r_1, \tag{6}$$

$$V = \frac{V_0}{\phi^2} + \frac{V_1}{\phi} + V_2, \tag{7}$$

$$U = \frac{U_0}{\phi^2} + \frac{U_1}{\phi} + U_2. \tag{8}$$

Considering a vacuum solution for the physical fields,

$$q_1 = 0, \qquad r_1 = 0. \tag{9}$$

The potentials V and U can be driven by lower dimensional arbitrary functions of space and time of the form (after substituting the vacuum solutions)

$$V_2 = V_2(y,t), \quad U_2 = U_2(x,t). \tag{10}$$

We now substitute the Bäcklund transformation (5)–(8) with the above choice of $\{q_1, r_1, V_2, U_2\}$ into (1)–(4) to obtain by collecting the coefficients of ϕ^{-3},

$$\lambda U_0 = \phi_x^2, \quad \lambda V_0 = \phi_y^2, \quad \lambda q_0 r_0 = \phi_x \phi_y. \tag{11}$$

Collecting the coefficients of ϕ^{-2}, we obtain the following set of equations:

$$-\mathrm{i}q_0\phi_t - 2q_{0x}\phi_x - q_0\phi_{xx} - 2q_{0y}\phi_y - q_0\phi_{yy} - 2\lambda q_0[U_1+V_1] = 0, \tag{12}$$

$$\mathrm{i}r_0\phi_t - 2r_{0x}\phi_x - r_0\phi_{xx} - 2r_{0y}\phi_y - r_0\phi_{yy} - 2\lambda r_0[U_1+V_1] = 0, \tag{13}$$

$$V_{0x} - V_1\phi_x = [q_0 r_0]_y, \tag{14}$$

$$U_{0y} - U_1\phi_y = [q_0 r_0]_x. \tag{15}$$

Solving the above set of overdetermined equations consistently, we obtain

$$V_1 = \frac{\phi_y\phi_{xx} - \phi_x\phi_{yy}}{\lambda\phi_x}, \tag{16}$$

$$U_1 = \frac{\phi_x\phi_{xy} - \phi_{xx}\phi_y}{\lambda\phi_y}. \tag{17}$$

Now, collecting the coefficients of ϕ^{-1}, we obtain the following set of equations:

$$\mathrm{i}q_{0t} + q_{0xx} + q_{0yy} - 2\lambda q_0[U_2+V_2] = 0, \tag{18}$$

$$-\mathrm{i}r_0 t + r_{0xx} + r_{0yy} - 2\lambda r_0[U_2+V_2] = 0, \tag{19}$$

$$V_{1x} = 0, \tag{20}$$

$$U_{1y} = 0. \tag{21}$$

The compatibility of the above equations requires that the manifolds ϕ and q_0 should evolve as

$$\phi(x,y,t) = \phi_1(x,t) + \phi_2(y,t), \tag{22}$$

$$r_0(x,y,t) = q_1(x,t)q_2(y,t). \tag{23}$$

From the Painlevé analysis of the (2+1)-dimensional AKNS system, we know that the resonance at $r = -1$ represents the arbitrariness of the manifold and this is indeed reflected by (22), while the resonance at $r = 0$ represents the arbitrariness of either q_0 or r_0 which is in line with (23).

3. Solutions of the (2+1)-Dimensional AKNS Equation and their Interactions

Thus, the physical fields of the (2+1)-dimensional AKNS equation can be explicitly given as

$$q = \frac{q_1(x,t)q_2(y,t)}{\phi_1(x,t)+\phi_2(y,t)}, \tag{24}$$

$$r = \frac{\phi_{1x}\phi_{2y}}{\lambda q_1(x,t)q_2(y,t)(\phi_1(x,t)+\phi_2(y,t))}, \tag{25}$$

while the potentials U and V can also be solved in terms of the arbitrary functions $\phi_1(x,t)$, $\phi_2(x,t)$, $q_1(x,t)$, $q_2(y,t)$ and $c(t)$:

$$U = -\frac{1}{\lambda}\{\ln[\phi_1(x,t)+\phi_2(y,t)]\}_{xx} + \frac{\mathrm{i}q_{1t}(x,t) + q_{1xx}(x,t) - c(t)q_1(x,t)}{2\lambda q_1(x,t)}, \tag{26}$$

$$V = -\frac{1}{\lambda}\{\ln[\phi_1(x,t)+\phi_2(y,t)]\}_{yy} + \frac{\mathrm{i}q_{2t}(y,t) + q_{2yy}(y,t) + c(t)q_2(y,t)}{2\lambda q_2(y,t)}. \tag{27}$$

The presence of the two-dimensional arbitrary functions presents the freedoms to generate a wide class of solutions of the (2+1)-dimensional AKNS equation. From the above, we find that the physical quantity "qr" takes the form

$$qr = \frac{\phi_{1x}\phi_{2y}}{\lambda(\phi_1(x,t)+\phi_2(y,t))^2}. \tag{28}$$

In (1+1)-dimensions, a single soliton can be found from the limiting case of a related periodic solution

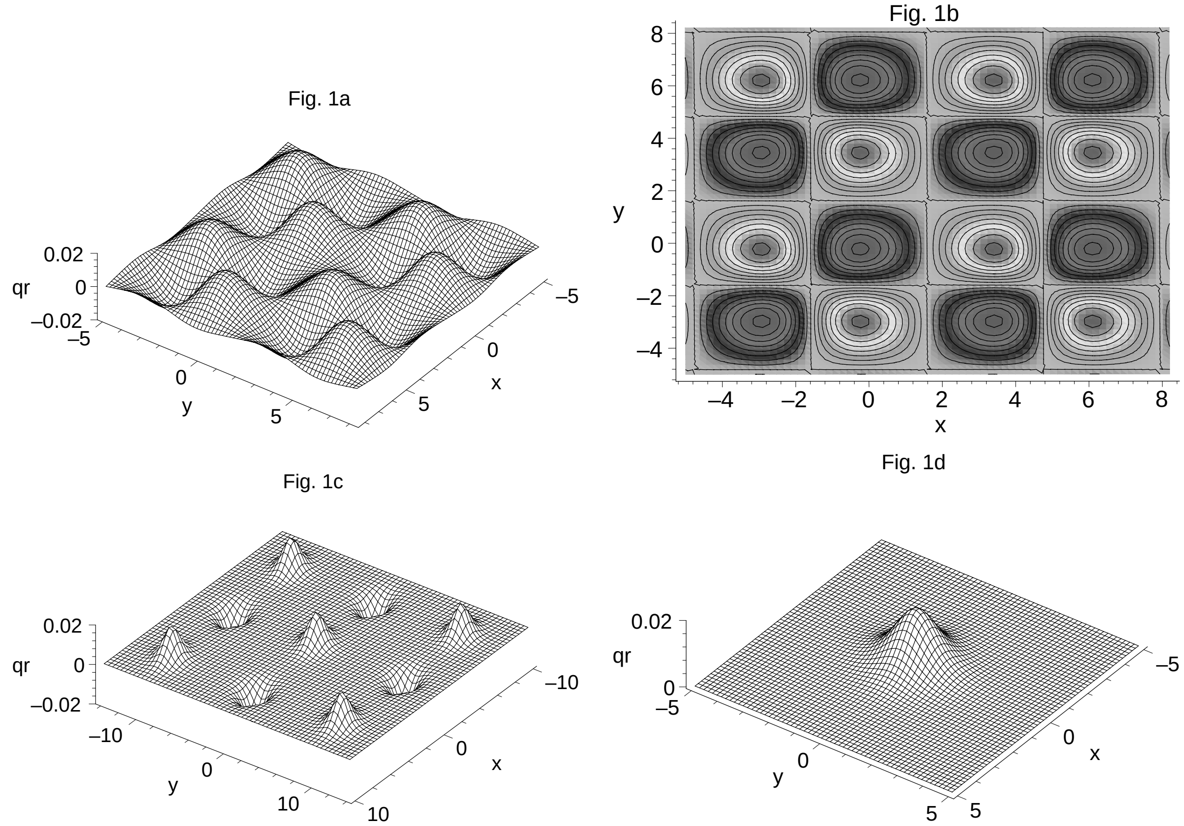

Fig. 1. (a) A plot of the periodic solution (28) for the choices given by (29), (30) and (31). (b) The contour plot of the periodic wave shown by (a). (c) The dromion lattice with $m_1 = 0.99$, $m_2 = 0.9995$. (d) A single dromion for the same choice given by (28), (29) and (30) with $m_1 = m_2 = 1$.

expressed by Jacobi elliptic functions. To generate a one-dromion solution for the quantity qr, which can be related to the energy of the system, we now drive the arbitrary function by Jacobi elliptic functions.

For instance, if we choose

$$\phi_1(x,t) = a_0 + a_1 \mathrm{sn}(k_1 x - \omega_1 t, m_1), \tag{29}$$

$$\phi_2(y,t) = a_2 \mathrm{sn}(k_2 y - \omega_2 t, m_2), \ |a_0| > |a_1| + |a_2|, \tag{30}$$

we obtain the one dromion of the AKNS system in terms of the Jacobian elliptic function. Figure 1a is a snapshot of the periodic solution (28) under the above choice of arbitrary functions with the following parameters:

$$\begin{aligned} &a_0 = 8, \quad a_1 = a_2 = k_1 = k_2 = \lambda = 1, \\ &\omega_1 = 2, \quad \omega_2 = 0, \quad m_1 = 0.2, \quad m_2 = 0.3 \end{aligned} \tag{31}$$

at time $t = 0$. Figure 1b is a contour plot of Figure 1a. When m_1 and m_2 approach unity, we get a dromion lattice solution given by Fig. 1c for the same parametric choice except that $m_1 = 0.99$, $m_2 = 0.9995$. Finally, when $m_1 = m_2 = 1$, the dromion lattice tends to a single dromion which is described by (28) with

$$\phi_1(x,t) = a_0 + a_1 \tanh(k_1 x - \omega_1 t), \tag{32}$$

$$\phi_2(y,t) = a_2 \tanh(k_2 y - \omega_2 t), \quad |a_0| > |a_1| + |a_2|, \tag{33}$$

and is shown in Fig. 1d at $t = 0$. Thus, we find that the exponentially localized dromions found earlier by Boiti et al. [1] appear only as a special case of the solutions driven by Jacobian elliptic functions.

The above analysis can be easily extended to generate multiple periodic wave solutions unlike (1+1)-dimensions where multiple soliton solutions can not be obtained from a limiting case of multiple periodic wave solutions expressed by means of the Jacobi elliptic functions. However, one can find many kinds of multiple periodic solutions in (2+1)-dimensions which are the generalizations of the different types of multi-dromions.

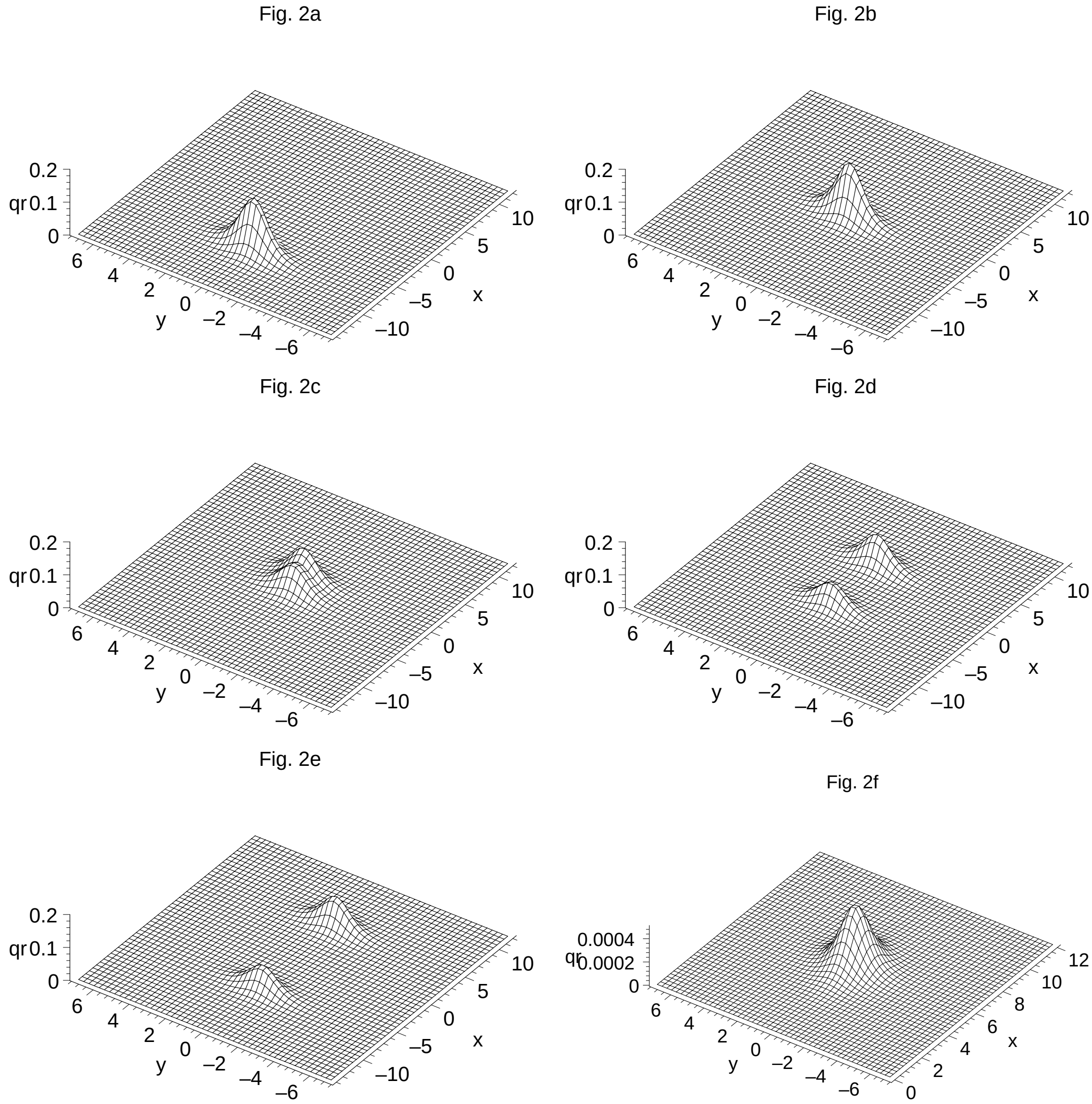

Fig. 2. Approximate dromion fission at times: (a) $t = -3$; (b) $t = 0$; (c) $t = 0.7$; (d) $t = 2$; (e) $t = 3$. (f) The tiny dromion at time $t = -3$ which is not observed in Fig. 1a as its amplitude is much smaller than that of the bigger one.

For instance, the choice

$$\phi_1(x,t) = a_0 + \sum_{i=1}^{N} a_i \mathrm{sn}^{c_i}(k_i x - \omega_i t, m_i), \quad c_i > 0, \quad d_i > 0, \tag{34}$$

$$\phi_2(y,t) = a_3 \sum_{i=1}^{M} b_i \mathrm{sn}^{d_i}(K_i y - \Omega_i t, \mu_i), \quad |a_0| > \sum_{i=1}^{N} |a_i| + \sum_{i=1}^{M} |b_i| \tag{35}$$

generates $(M+N)$ periodic wave interaction solutions which are the generalization of an $M \times N$ dromion solution.

It is known that localized excitations in higher dimensions undergo both elastic and inelastic collisions. Two localized excitations may exchange their physical quantities such as the energy and the momentum. Two solitons (or solitary waves) may fuse together to form one soliton, and one soliton may split into two solitons. To bring out a deeper understanding on the interaction of dromions, we take a two-dromion solution of the AKNS system with the following choices of the arbi-

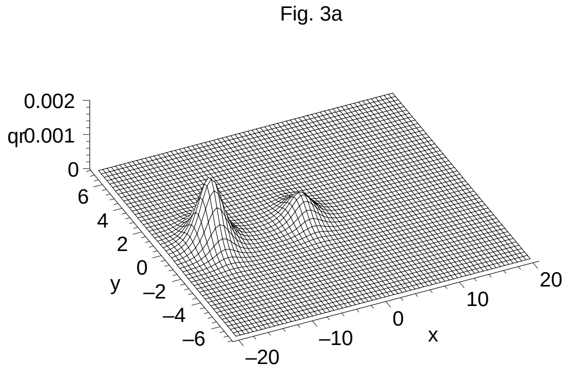

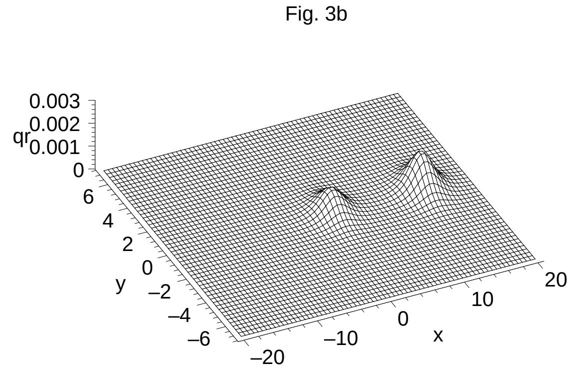

Fig. 3. The pursuant dromion interaction: (a) before the interaction at time $t = -3.5$; (b) after the interaction at $t = 3.5$.

trary functions:

$$\phi_1(x,t) = a_0 + a_1 \tanh(k_1 x - \omega_1 t) + a_2 \tanh(k_2 x + \omega_2 t), \quad (36)$$

$$\phi_2(y,t) = a_3 \tanh(k_3 y - \omega_3 t), \quad |a_0| > |a_1| + |a_2| + |a_3|. \quad (37)$$

Before we give a detailed analytical analysis of the interaction of dromions, we first discuss them numerically.

Figure 2 shows the evolution of the two-dromion solution (28) with (36) and (37) and the parametric choice

$$a_0 = 24, \quad a_1 = 20, \quad a_2 = a_3 = k_1 = k_2 = k_3 = 1, \quad \omega_1 = 2, \quad \omega_2 = -2, \quad \lambda = 1 \quad (38)$$

at times $t = -3$, 0, 0.7, 2 and 3, respectively.

From Figs. 2a and 2b, we observe only one dromion. From Figs. 2c – 2e, we find that one dromion splits into two. This phenomenon is known as dromion (or soliton) fission. However, this observation may not be exactly correct at least for the (2+1)-dimensional AKNS system. Actually, before the interaction, there are two dromions. While one is explicitly visible, the other is relatively too small as to observe it explicitly. If we search and focus on a region far away from the bigger dromion, we can recover the smaller one. Figure 2f shows that before the interaction (at $t = -3$), a smaller dromion does really exist with the amplitude ~ 0.0005, while the amplitude of the bigger one is about 0.2. Strictly speaking, after the interaction, the tiny dromion obtains energy from the bigger one and becomes visible. From this, one can conclude that the dromion fission may be considered only as an approximate phenomenon.

Different choices of the constant parameters in (36) and (37) may lead to different inelastic collision phenomena. Figure 3 shows the inelastic pursuant dromion interaction and illustrates how they evolve in time exchanging energy among themselves, while Fig. 2 displays a head on collision of dromions.

To bring out the exchange interaction [13] where the interacting dromions completely exchange their shapes, we again consider the two-dromion solution (28) with (36) and (37) and choose the parameters as

$$a_0 = 24, \quad a_1 = a_2 = a_3 = k_1 = k_2 = k_3 = 1, \quad \omega_1 = 2, \quad \omega_2 = -2, \quad \lambda = 1. \quad (39)$$

From Figs. 4a and 4c, one finds that the left moving dromion after the interaction ($t = 2.5$) possesses the shape of the right moving dromion before the interaction ($t = -2.5$) and vice versa. This conclusion can be strictly proved analytically later.

Figure 5 brings out the fusion of two dromions. Before the interaction (Fig. 5a), there are two explicit dromions. After the interaction (Fig. 5c), we observe only one dromion and we call this phenomenon as dromion (or soliton) fusion. It must be emphasized that the concept of fusion is again an approximate phenomenon like fission with reference to the (2+1)-dimensional AKNS system as the tiny dromion with amplitude ~ 0.0005 can be made visible by searching far away from the domain of the bigger dromion (Fig. 5f).

The interaction discussed so far is inelastic in nature. To bring out the multi-dromion elastic interaction, we choose the arbitrary functions as

$$\phi_1(x,t) = a_0 + a_1 \operatorname{sech}(k_1 x - \omega_1 t) + a_2 \operatorname{sech}(k_2 x + \omega_2 t), \quad (40)$$

Fig. 4a

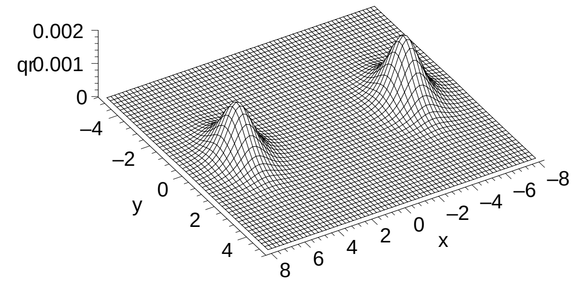

Fig. 4b

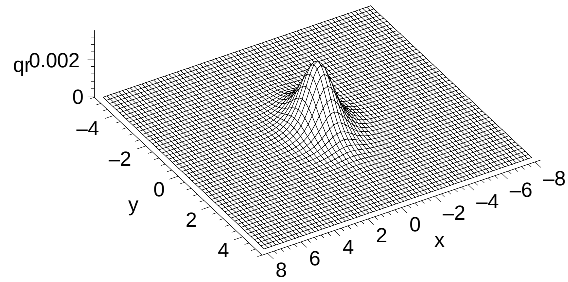

Fig. 4c

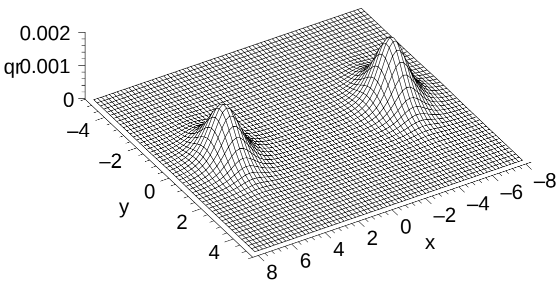

Fig. 4. The exchange dromion interaction at times: (a) $t = -2.5$; (b) $t = 0$; (c) $t = 2.5$.

Fig. 5a

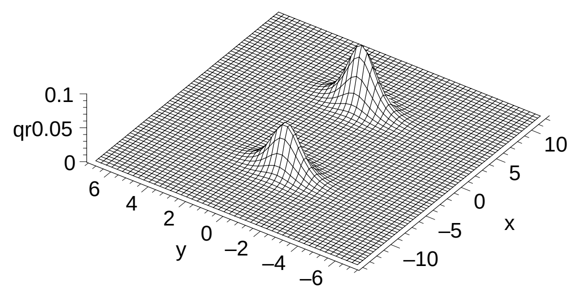

Fig. 5b

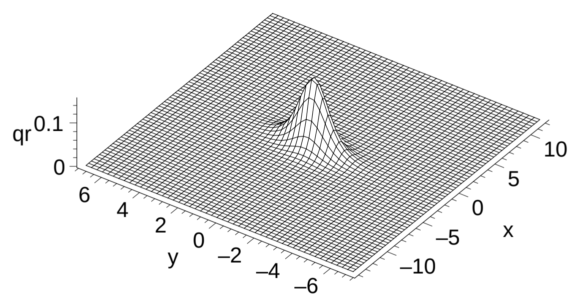

Fig. 5c

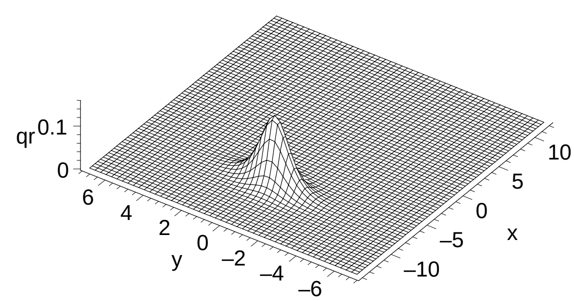

Fig. 5d

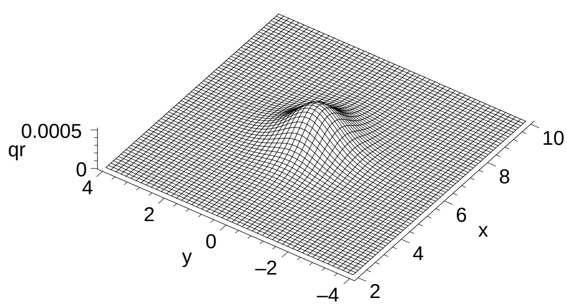

Fig. 5. The approximate fusion interaction of dromions at times: (a) $t = -3$; (b) $t = 0$; (c) $t = 3$. (d) A tiny dromion after the interaction at $t = 3$.

Fig. 6a

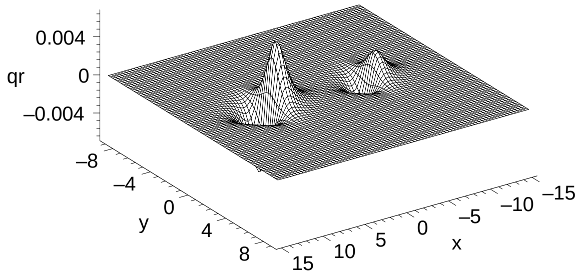

Fig. 6b

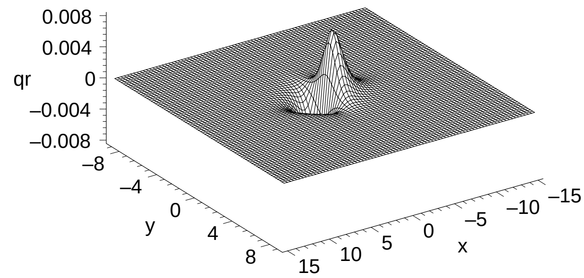

Fig. 6c

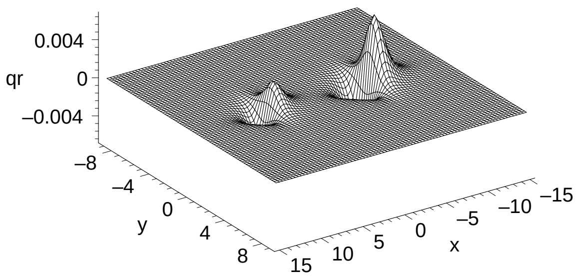

Fig. 6. The completely elastic interaction of dipole-type dromions at times: (a) $t = -3$; (b) $t = 0$; (c) $t = 3$.

$$\phi_2(y,t) = a_3 \tanh(k_3 y - \omega_3 t). \tag{41}$$

Figure 6 shows elastic interaction of the dipole-type dromions (with positive and negative amplitude) given by (28) with (40) and (41) for the parametric choice

$$\begin{aligned} &a_0 = 13, \quad a_1 = a_3 = k_1 = k_2 = k_3 = 1, \\ &a_2 = 3, \quad \omega_1 = 2, \quad \omega_2 = -2, \quad \lambda = 1. \end{aligned} \tag{42}$$

The above numerical results can also be proved analytically by carrying out the asymptotic analysis of the expression given by (28) with (36) and (37) or (40) and (41).

Without loss of generality, we can always assume that $k_1 > 0$ and $k_2 > 0$ in (36) and (40) as $\tanh(x)$ is an odd function of x and $\mathrm{sech}(x)$ is an even function, while a_1 and a_2 are arbitrary constants. Assuming that

$$\frac{\omega_2}{k_2} < \frac{\omega_1}{k_1},$$

it is straightforward to find that for the two-dromion solution (28) with (36) and (37), we have

$$\begin{aligned} qr_- &\equiv qr_{t\to-\infty} = \\ &\frac{a_1 k_1 a_3 k_3 \mathrm{sech}^2(k_1 x - \omega_1 t)\mathrm{sech}^2(k_3 y)}{(a_0 - a_2 + a_1 \tanh(k_1 x - \omega_1 t) + a_3 \tanh(k_3 y))^2} + \frac{a_2 k_2 a_3 k_3 \mathrm{sech}^2(k_2 x - \omega_2 t)\mathrm{sech}^2(k_3 y)}{(a_0 + a_1 + a_2 \tanh(k_2 x - \omega_2 t) + a_3 \tanh(k_3 y))^2}, \end{aligned} \tag{43}$$

$$\begin{aligned} qr_+ &\equiv qr_{t\to+\infty} = \\ &\frac{a_1 k_1 a_3 k_3 \mathrm{sech}^2(k_1 x - \omega_1 t)\mathrm{sech}^2(k_3 y)}{(a_0 + a_2 + a_1 \tanh(k_1 x - \omega_1 t) + a_3 \tanh(k_3 y))^2} + \frac{a_2 k_2 a_3 k_3 \mathrm{sech}^2(k_2 x - \omega_2 t)\mathrm{sech}^2(k_3 y)}{(a_0 - a_1 + a_2 \tanh(k_2 x - \omega_2 t) + a_3 \tanh(k_3 y))^2}, \end{aligned} \tag{44}$$

while for the two-dipole-type-dromion solution (28) with (40) and (41), we obtain

$$\begin{aligned} qr_\pm &\equiv qr_{t\to\pm\infty} = \\ &\frac{a_1 k_1 a_3 k_3 \mathrm{sech}^2(k_1 x - \omega_1 t)\tanh(k_1 x - \omega_1 t)\mathrm{sech}^2(k_3 y)}{(a_0 + a_1 \mathrm{sech}(k_1 x - \omega_1 t) + a_3 \tanh(k_3 y))^2} + \frac{a_2 k_2 a_3 k_3 \mathrm{sech}^2(k_2 x - \omega_2 t)\tanh(k_2 x - \omega_2 t)\mathrm{sech}^2(k_3 y)}{(a_0 + a_2 \mathrm{sech}(k_2 x - \omega_2 t) + a_3 \tanh(k_3 y))^2}. \end{aligned} \tag{45}$$

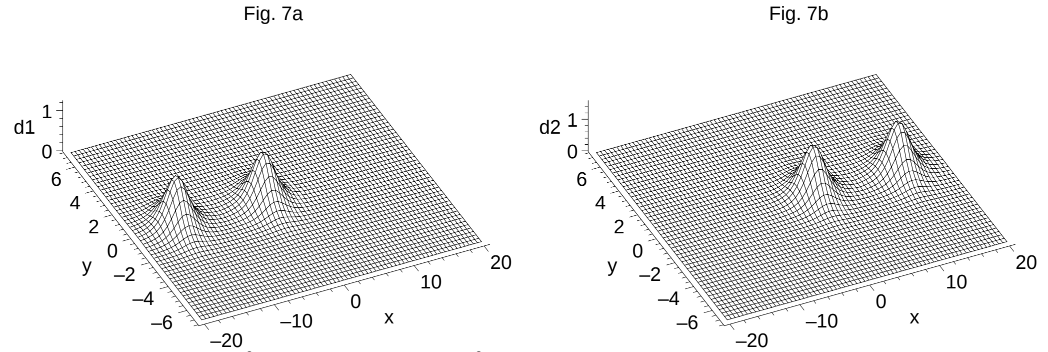

Fig. 7. The error plots of $d1 \equiv 10^9|qr - qr_-|$ and $d2 \equiv 10^9|qr - qr_+|$ at times: (a) $t = -3.5$ and (b) $t = 3.5$ related to Figure 3.

For the dipole-dromion interaction, the elastic interaction occurs by virtue of the asymptotic behavior of (45).

For the two-dromion solution (28) with (36) and (37), we first write down the amplitudes of the dromions before and after interaction. Before the interaction, the amplitude for the faster moving dromion (we assume right moving is faster than left moving) is given by

$$A_{1-} = \frac{|a_1 a_3 k_1 k_3|}{(a_0 - a_2)^2}, \tag{46}$$

while for the slower moving dromion, we have the amplitude given by

$$A_{2-} = \frac{|a_2 a_3 k_2 k_3|}{(a_0 + a_1)^2}. \tag{47}$$

After the interaction, the amplitudes are

$$A_{1+} = \frac{|a_1 a_3 k_1 k_3|}{(a_0 + a_2)^2} \tag{48}$$

for the faster moving dromion and

$$A_{2+} = \frac{|a_2 a_3 k_2 k_3|}{(a_0 - a_1)^2} \tag{49}$$

for the slower moving dromion, respectively.

From the expression for the amplitudes, we observe that the "approximate" fission phenomenon is related to

$$\frac{A_{1-}}{A_{2-}} = \frac{a_1 k_1 (a_0 + a_1)^2}{a_2 k_2 (a_0 - a_2)^2} \gg 1, \text{ or } \frac{A_{1-}}{A_{2-}} \ll 1, \tag{50}$$

while the "approximate" fusion phenomenon will be observed when

$$\frac{A_{1+}}{A_{2+}} = \frac{a_1 k_1 (a_0 - a_1)^2}{a_2 k_2 (a_0 + a_2)^2} \gg 1, \text{ or } \frac{A_{1+}}{A_{2+}} \ll 1. \tag{51}$$

Figures 2 and 5 correspond to the cases (50) and (51), respectively.

If the conditions

$$A_{1+} = A_{2-}, \quad A_{2+} = A_{1-}, \quad k_1 = k_2 \tag{52}$$

are satisfied, then we obtain the exchange interaction shown in Figure 4.

To see the accuracy of the approximate expressions, we plot down the quantities

$$d1 \equiv 10^9|qr - qr_-| \text{ and } d2 \equiv 10^9|qr - qr_+|$$

in Fig. 7 for the inelastic pursuant collision corresponding to Figure 3. Figure 7 shows that the errors between the exact solution and asymptotic expressions are only about 10^{-9}.

From (24)–(27), we find that two more arbitrary functions $q_1(x,t)$ and $q_2(y,t)$ have been included in exact solutions unlike the solutions obtained from the multilinear variable separation approach [12]. These arbitrary functions have no effect on the quantity qr while their effect on the potentials will have to be investigated. Figure 8 displays the structures of the potential V for the choice of q_1 and $c(t)$ as

$$q_1 = 4 + \tanh(x + 2t), \quad c(t) = \mathrm{e}^{-t}, \tag{53}$$

while all the other parameters and arbitrary functions are the same as in the case of Figure 1d. Figures 8a–8c show the evolution of the real parts of V while Fig. 8d exhibits the structure of the imaginary parts of V. From Fig. 8, we observe that the arbitrary function q_1 may generate new line solitons for the potential V.

4. Summary and Discussion

In this paper, we have formulated a new method to construct the solutions of the (2+1)-dimensional

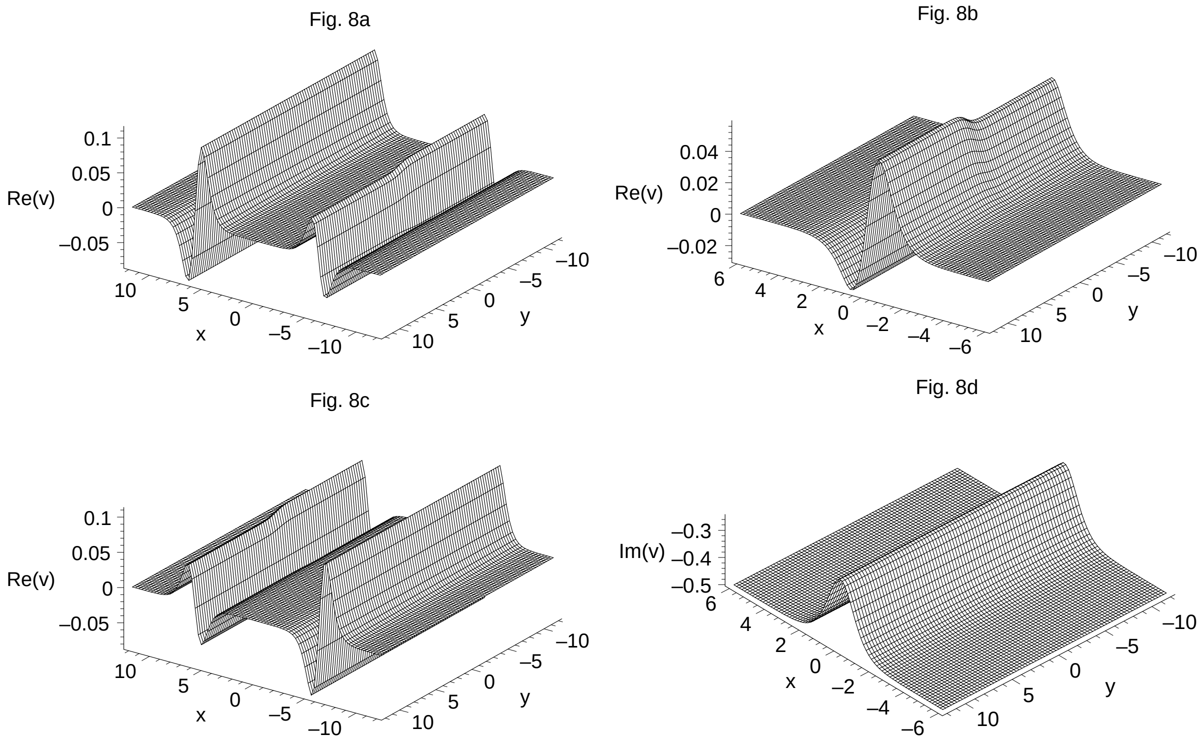

Fig. 8. The time evolution of the real part of the potential V given by (27) with (32), (33) and (53) at times: (a) $t = -3$; (b) $t = 0$; (c) $t = 3$. (d) The corresponding structure of the imaginary part of the potential V at $t = 0$.

AKNS system by suitably harnessing the results of the Painlevé analysis. This method which is more elegant and straightforward gives us an unprecedented possibility of constructing a wide class of solutions of (2+1)-dimensional soliton equations.

We have obtained abundant localized exact solutions and studied interaction properties among different types of localized excitations. We also observed that the dromion interactions may be elastic or inelastic. When the interaction is inelastic, two dromions may exchange their physical quantities partially and may completely exchange their shapes. Contrary to the traditional viewpoint, we emphasized that the concept of fission (or fusion) of dromions may be an approximate phenomenon at least with reference to the (2+1)-dimensional AKNS system.

We have also obtained multiple periodic wave solutions which may degenerate to multiple dromions just as *one* soliton can be obtained as the limiting case of Jacobi elliptic function in (1+1)-dimensions.

The investigation of the other well-known (2+1)-dimensional soliton equations using the Painlevé truncation method is under progress and the results will be published later.

Acknowledgement

The work was supported by the National Natural Science Foundations of China (No. 90203001, No. 10475055 and No. 90503006).

[1] M. Boiti, J. J. P. Leon, M. Manna, and F. Pempinelli, Phys. Lett. A **132**, 432 (1986).

[2] A. S. Fokas and P. M. Santini, Physica D **44**, 99 (1990); J. Hietarinta, Phys. Lett. A **149**, 133 (1990).

[3] R. Radha and M. Lakshmanan, J. Math. Phys. **35**, 4746 (1994).

[4] S. Y. Lou, J. Phys. A: Math. Gen. **28**, 7227 (1995); S. Y. Lou, J. Phys. A: Math. Gen. **29**, 5989 (1996).

[5] W. S. Duan, B. R. Wang, and R. J. Wei, Phys. Rev. E **55**, 1773 (1997); G. I. Stegeman and M. Segev, Science **286**, 1518 (1999); R. A. Battye and P. M. Sutcliffe, Nucl. Phys. B **590**, 329 (2000); S. Wang, X. Y Tang,

and S. Y. Lou, Chaos, Solitons and Fractals **21**, 231 (2004); V. A. Aleshkevich, Y. V. Kartashov, A. S. Zelenina, V. A. Vysloukh, J. P. Torres, and L. Torner, Opt. Lett. **29**, 483 (2004); A. K. Abeeluck and C. Headley, Opt. Lett. **30**, 61 (2005); F. Lu, Q. Lin, W. H. Knox, and G. P. Agrawal, Phys. Rev. Lett. **93**, 183901 (2004); Y. V. Kartashov, L. C. Crasovan, A. S. Zelenina, V. A. Vysloukh, A. Sanpera, M. Lewenstein, and L. Torner, Phys. Rev. Lett. **93**, 143902 (2004).

[6] W. Krolikowski and S. A. Holmstrom, Opt. Lett. **22**, 369 (1997); S. N. M. Ruijsenaars, Ann. Phys. **256**, 226-301 (1997); V. V. Steblina and Y. S. Kivshar, Opt. Lett. **23**, 156 (1998); Z. H. Musslimani, M. Soljacic, M. Segev, and D. N. Christodoulides, Phys. Rev. Lett. **86**, 799 (2001); M. J. Ablowitz and Z. H Musslimani, Phys. Rev. E **65**, 056618 (2002); X. Y. Tang and S. Y Lou, Chin. Phys. Lett. **20**, 335 (2003); B. B. Baizakov, B. A. Malomed, and M. Salerno, Phys. Rev. A **70**, 053613 (2004).

[7] M. J. Ablowitz and R. Haberman, Phys. Rev. Lett. **35**, 1185 (1975).

[8] A. S. Fokas, Phys. Rev. Lett. **51**, 3 (1983).

[9] A. S. Fokas and M. J. Ablowitz, J. Math. Phys. **25**, 2494 (1984).

[10] K. Nishinari and J. Satsuma, J. Phys. Soc. Jpn. **62**, 2021 (1993).

[11] S. Y. Lou, C.-L. Chen, and X. Y. Tang, J. Math. Phys. **43**, 4078 (2002).

[12] S. Y. Lou, X. Y. Tang, and J. Lin, J. Math. Phys. **41**, 8286 (2000); G. Saccomandi, J. Math. Phys. **30**, 2211 (1997); P. A Clarkson, Chaos, Solitons and Fractals **5**, 2261 (1995).

[13] X. Y. Tang, S. Y. Lou, and Y. Zhang Phys. Rev. E **66**, 046601 (2002); X. Y. Tang and S. Y. Lou, J. Math. Phys. **44**, 4000 (2003); H. C. Hu, X. Y. Tang, S. Y. Lou, and Q. P. Liu, Chaos, Solitons and Fractals **22**, 327 (2004); S. Y. Lou, Phys. Lett. A **277**, 94 (2000); S. Y. Lou and H. Y. Ruan, J. Phys. A **34**, 305 (2001).